Available online at www.sciencedirect.com

ScienceDirect

Mendeleev Commun., 2024, **34**, 653–655

Mendeleev Communications

Kinetics of N_2O decomposition over bulk and supported $LaCoO_3$ perovskites

Petr V. Zemlianskii,*[a] Alexander L. Kustov,[a,b] Gennady I. Kapustin,[a] Nikolay A. Davshan,[a] Konstantin B. Kalmykov,[b] Vladimir V. Chernyshev[b] and Leonid M. Kustov[a,b]

[a] *N. D. Zelinsky Institute of Organic Chemistry, Russian Academy of Sciences, 119991 Moscow, Russian Federation. E-mail: petrzemlianskii@gmail.com*

[b] *Department of Chemistry, M. V. Lomonosov Moscow State University, 119991 Moscow, Russian Federation*

DOI: 10.1016/j.mencom.2024.09.009

For the first time, kinetic data on the decomposition of N_2O over mixed oxide $LaCoO_3$ with a perovskite structure have been obtained. Bulk $LaCoO_3$ synthesized using microwave activation exhibited an increased intrinsic reaction rate with a 30 kJ mol^{-1} lower activation energy. Perovskite samples supported on ZrO_2-La demonstrated lower intrinsic reaction rates due to the lower content of the $LaCoO_3$ phase, but the activation energies were also lower by 50–80 kJ mol^{-1}.

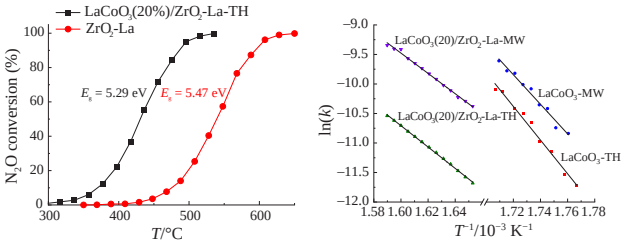

Keywords: microwave activation, bulk perovskite, supported perovskite, $LaCoO_3$, N_2O decomposition, kinetics, oxygen vacancies.

Nitrous oxide (N_2O) is known as a potent greenhouse gas, with a global warming potential 310 times greater than that of CO_2.[1,2] One of the main sources of emissions are nitric acid plants and particularly ammonia burners. A huge number of catalysts have been proposed for N_2O decomposition, such as metal-modified zeolites,[3–6] supported noble metals[7–9] and mixed oxides, especially, alkali-promoted Co spinels[10] and perovskites.[11–14] Low thermal and hydrothermal stability, as well as high cost, limit the industrial application of zeolites and noble metal-based catalysts. For this reason, perovskites are considered promising catalytic systems for N_2O decomposition due to their chemical stability at high temperatures and in the presence of water, as well as low cost.

It is known that microwave activation used in the synthesis of oxide materials is critical for increasing catalytic activity.[11,15] This is mainly due to the fast, uniform heating process. Fast heating can also lead to the formation of crystal lattice defects, which are oxygen vacancies in the case of perovskites. As the number of oxygen vacancies increases, so does the number of coordinatively unsaturated metal ions, which have been shown to be active centers of N_2O decomposition.[6]

N_2O decomposition was studied over $LaBO_3$ perovskites (B can be Fe, Co, Mn or Cr) synthesized by the Pechini method using citric acid[16] or urea.[17] It turned out that lanthanum cobaltite $LaCoO_3$, the only one of the entire series of perovskites synthesized using microwave activation,[18] has the best catalytic characteristics, although in a photocatalytic process, and not in the N_2O decomposition reaction, in which it, like supported $LaCoO_3$, was not investigated.

All things considered, in this work we investigated the effect of microwave activation during the synthesis of both bulk and supported $LaCoO_3$ on their catalytic performance in the process of N_2O decomposition. Particular attention was paid to the correlations between the concentration of oxygen vacancies and the intrinsic reaction rate, as well as the activation energy. Oxygen vacancy concentrations were compared using bandgap values from UV-VIS diffuse reflectance spectra.

Bulk and supported $LaCoO_3$ perovskites were prepared with and without microwave activation.† The microwave treatment time (5 min) was chosen according to Jung *et al.*[18] where a similar synthesis was performed, but using malic acid instead of glycine. The calcination step was necessary for two reasons. Firstly, the perovskite phase is formed only when the sample is calcined at temperatures above 500 °C.[18] Secondly, the decomposition of N_2O was carried out at temperatures up to 500–550 °C, so the catalysts used had to be stable under these conditions. A $LaCoO_3$ content of 20 wt% was chosen because supported $LaCoO_3$ perovskites with a content of 20% or higher are commonly used in catalysis due to their better performance.[20–22] A zirconia-based support was chosen as a

† The synthesis was carried out according to the procedure described elsewhere.[19] Briefly, aqueous solutions of lanthanum(III) and cobalt(II) nitrates (molar ratio 1 : 1) and glycine were prepared, and the molar ratio of glycine to ($La^{3+} + Co^{2+}$) was 5 : 1. Two portions (10 ml each) of the final mixture (40 ml in total) were poured into crucibles. The first crucible was placed in the center of a Midea AM720C4E-S household microwave oven. Microwave activation at a power of 900 W lasted 5 min without stirring or rotation the crucible. The resulting black foam was crushed and calcined in a muffle furnace at 600 °C for 5 h to obtain the calcination product $LaCoO_3$-MW. The second portion of the glycine complex was evaporated at 120 °C for 5 h to form black foam, which was calcined under the same conditions as in the case of microwave activation, thus obtaining the product $LaCoO_3$-TH. The remainder of the glycine complex (20 ml) was used for wet impregnation of ZrO_2-La. One part of the support was impregnated and dried under microwave activation conditions in a household oven for 5 min, while the other part was dried by thermal heating at 120 °C for 5 h. In both cases, such a volume of the glycine complex was added so that the $LaCoO_3$ content in the final catalyst was 20 wt%. The samples were then calcined in a muffle furnace at 600 °C for 5 h, yielding the final materials $LaCoO_3(20)/ZrO_2$-La-MW and $LaCoO_3(20)/ZrO_2$-La-TH, respectively.

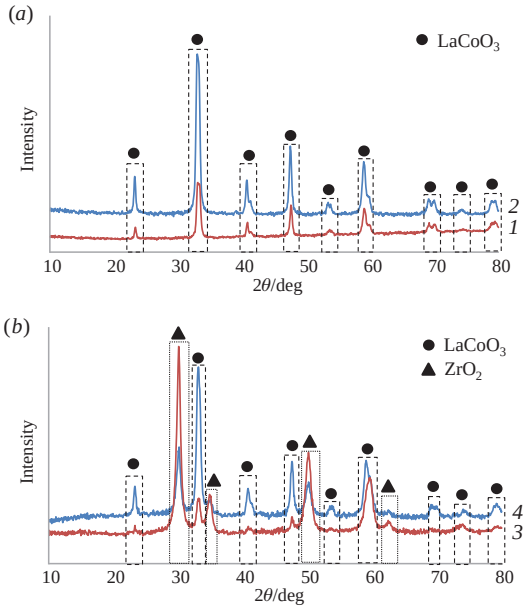

Figure 1 Powder X-ray diffraction patterns of (*a*) bulk and (*b*) supported $LaCoO_3$ materials: (*1*) $LaCoO_3$-MW and (*3*) $LaCoO_3(20)/ZrO_2$-La-MW synthesized with activation by microwave heating, as well as (*2*) $LaCoO_3$-TH and (*4*) $LaCoO_3(20)/ZrO_2$-La-TH synthesized by conventional thermal heating.

model commercial support from Saint-Gobain. Supported perovskites $LaBO_3/ZrO_2$ (B is Fe, Co and Ni) were previously investigated by us in the oxidation of CO.[19]

Powder X-ray diffraction patterns (Figure 1) confirmed that the materials synthesized under both microwave treatment and conventional thermal heating conditions were $LaCoO_3$ and $LaCoO_3/ZrO_2$ in accordance with JCPDS-ICDD 00-048-0123 for $LaCoO_3$ and JCPDS-ICDD 00-049-1642 for ZrO_2. It is worth noting that samples obtained using thermal heating have higher crystallinity compared to samples synthesized using microwave activation.

TEM photographs (Figure S2, see Online Supplementary Materials) showed that $LaCoO_3$-TH was composed of smaller agglomerates with a lower degree of sintering than $LaCoO_3$-MW, 50–54 and 70–72 nm, respectively. The presence of larger agglomerates in $LaCoO_3$-MW may be due to the fact that extremely fast heating occurs during microwave activation and hence faster crystal growth.[15,23,24]

According to SEM data (Figure S3 and Table 1), both $LaCoO_3(20)/ZrO_2$-La-TH and $LaCoO_3(20)/ZrO_2$-La-MW exhibit the same dispersion of the active phase on the ZrO_2 surface. Elemental mapping was carried out relative to cobalt, since lanthanum and oxygen were present in both the $LaCoO_3$ and ZrO_2-La phases.

Table 1 Data on the textural properties, particle sizes and band gaps of all synthesized samples.

Sample	Textural properties			TEM	SEM	
	A_{BET}/ $m^2\ g^{-1}$	V_Σ/ $cm^3\ g^{-1}$	D_{pore}/ nm	$D_{particle}$/ nm	$D_{particle}$/ μm	E_g/eV
$LaCoO_3$-TH	20	0.10	36.8	50–54		4.87
$LaCoO_3$-MW	16	0.11	37.6	70–72		4.80
$LaCoO_3(20)/ZrO_2$-La-TH	69	0.17	5.8		90[a]	5.29
$LaCoO_3(20)/ZrO_2$-La-MW	72	0.19	6.7		90[a]	5.27
ZrO_2-La	124	0.24	5.2		90	5.47

[a] The resolution of the SEM allowed only the size of the support particles to be correctly estimated.

Textural properties (see Table 1) demonstrate the following trends. The $LaCoO_3$-TH sample has a wider pore size distribution, more noticeably shifted towards the region of large mesopores and macropores, than in the case of the $LaCoO_3$-MW sample. This feature may lead to better accessibility of active sites in $LaCoO_3$-TH. Moreover, the $LaCoO_3$-TH sample has a 20% higher specific surface area compared to the $LaCoO_3$-MW sample, which may result in a better distribution of active sites. As for the supported catalysts, both $LaCoO_3(20)/ZrO_2$-La-TH and $LaCoO_3(20)/ZrO_2$-La-MW have approximately the same specific surface area, but the total pore volume of the $LaCoO_3(20)/ZrO_2$-La-MW sample is significantly higher than that of the $LaCoO_3(20)/ZrO_2$-La-TH sample. This is due to the fact that in the case of the $LaCoO_3(20)/ZrO_2$-La-MW sample, less $LaCoO_3$ phase is formed in the pore space of ZrO_2-La.

The band gap (E_g) values determined from the UV-VIS diffuse reflectance spectra (see Online Supplementary Materials) are summarized in Table 1. It can be seen that with the incorporation of the $LaCoO_3$ phase, a narrowing of the band gap occurs. This may be due to an increase in the concentration of oxygen vacancies. Both bulk and supported $LaCoO_3$ samples synthesized using microwave activation have narrower band gaps compared to the samples obtained without microwave treatment.

Details of the catalytic experiments are provided in Online Supplementary Materials. Arrhenius plots were calculated from N_2O conversion obtained during temperature-programmed experiments in the kinetic mode (α_{real} = 1–10%). The apparent activation energy values reported in Table 2 were calculated from the slope of the Arrhenius plots [Figure 2(*b*)].

For the Arrhenius plot, rate constants were used calculated from equation (1), where Q_0 is the total flow rate, α_{real} is the apparent N_2O conversion, and m is the catalyst loading equal to 0.1 g. Equation (1) is relevant for a flow reactor taking into account the first order kinetic reaction.[16]

$$k = \frac{Q_0}{m} \ln\left(\frac{1}{1-\alpha_{real}}\right) \quad (1)$$

The intrinsic reaction rate was calculated using equation (2), where F_{N_2O} refers to the molar flow rate of N_2O at the reactor inlet.

$$r = k \frac{F_{N_2O}\ \alpha_{real}}{A_{BET}\ Q_0} \quad (2)$$

Table 2 Results of kinetic experiments using synthesized catalysts.

Catalyst	Intrinsic reaction rate[a]/ (mol N_2O) $m^{-2}\ h^{-1}$	Apparent activation energy/kJ mol^{-1}
$LaCoO_3$-TH	4.4×10^{-9}	237
$LaCoO_3$-MW	1.4×10^{-8}	208
$LaCoO_3(20)/ZrO_2$-La-TH	8.4×10^{-11}	150
$LaCoO_3(20)/ZrO_2$-La-MW	9.5×10^{-10}	143

[a] Measured at 313 °C for the bulk catalysts and at 336 °C for the supported ones.

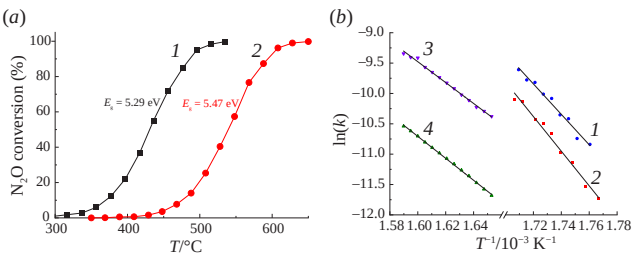

Figure 2 (*a*) Temperature curves of N_2O conversion over (*1*) $LaCoO_3(20)/ZrO_2$-La-TH and (*2*) blank ZrO_2-La. (*b*) Arrhenius plots for all synthesized catalysts: (*1*) $LaCoO_3$-MW, (*2*) $LaCoO_3$-TH, (*3*) $LaCoO_3(20)/ZrO_2$-La-MW and (*4*) $LaCoO_3(20)/ZrO_2$-La-TH.

As can be seen in Figure 2(*a*), blank ZrO_2-La was significantly less active in N_2O decomposition than $LaCoO_3(20)/ZrO_2$-La-TH. Thus, the perovskite phase made the main contribution to the catalytic performance. This was probably due to a narrowing of the band gap (see Table 1), which indirectly indicated an increase in the concentration of oxygen vacancies. It turned out that the $LaCoO_3$-MW and $LaCoO_3(20)/ZrO_2$-La-MW samples have higher catalytic activity in the decomposition of N_2O compared to $LaCoO_3$-TH and $LaCoO_3(20)/ZrO_2$-La-TH, respectively, as evidenced by higher intrinsic reaction rates (see Table 2). It was also observed that the supported $LaCoO_3$ samples were less active due to the lower content of the $LaCoO_3$ phase. It should be noted that the supported samples made it possible to reduce the activation energy of N_2O decomposition compared to the bulk samples.

In this work, we showed for the first time the effect of activation by microwave heating on the structural and textural properties of $LaCoO_3$ and $LaCoO_3(20)/ZrO_2$-La and, consequently, on the catalytic activity in the decomposition of N_2O. It was revealed that treatment with microwave heating followed by calcination in a muffle furnace leads to the formation of $LaCoO_3$, consisting of larger agglomerates with a higher degree of sintering compared to $LaCoO_3$ synthesized without microwave activation. Microwave activation also resulted in a narrower pore size distribution, fewer narrow mesopores and a 20% reduction in specific surface area. The $LaCoO_3(20)/ZrO_2$-La-MW sample also had a higher total pore volume due to less filling of the pore space with the resulting perovskite phase. It was demonstrated that the formation of the $LaCoO_3$ phase on the ZrO_2-La surface leads to a narrowing of the band gap, probably due to an increase in the concentration of oxygen vacancies. This resulted in a shift of the conversion curve to the region of lower temperatures. Microwave activation at the synthesis stage led to an increase in the intrinsic reaction rate for both bulk and supported $LaCoO_3$, as well as a decrease in the activation energy by 30 kJ mol^{-1} in the case of bulk $LaCoO_3$. The perovskite samples supported on ZrO_2-La demonstrated lower intrinsic reaction rates due to the lower content of the $LaCoO_3$ phase, but the activation energies were also lower by 50–80 kJ mol^{-1}. The improvement of the catalytic activity for the samples synthesized using microwave activation may be associated with a narrowing of the band gap, which is probably indirect evidence of an increase in the concentration of oxygen vacancies.

This work was supported by the Russian Science Foundation (project no. 23-73-30007).

Online Supplementary Materials

Supplementary data associated with this article can be found in the online version at doi: 10.1016/j.mencom.2024.09.009.

References

1 J. Pérez-Ramirez, F. Kapteijn, K. Schöffel and J. A. Moulijn, *Appl. Catal., B*, 2003, **44**, 117.
2 P. Granger and V. I. Parvulescu, *Chem. Rev.*, 2011, **111**, 3155.
3 M. C. Campa, D. Pietrogiacomi, C. Catracchia, S. Morpurgo, J. Olszowka, K. Mlekodaj, M. Lemishka, J. Dedecek, A. Kornas and E. Tabor, *Appl. Catal., B*, 2024, **342**, 123360.
4 B. Kang, M. Li, Z. Di, X. Guo, Y. Wei, J. Jia and R. Zhang, *Catal. Today*, 2022, **402**, 17.
5 F. Lin, T. Andana, Y. Wu, J. Szanyi, Y. Wang and F. Gao, *J. Catal.*, 2021, **401**, 70.
6 L. M. Kustov, S. F. Dunaev and A. L. Kustov, *Molecules*, 2022, **27**, 398.
7 M. C. Campa, G. Fierro, A. M. Doyle, S. Tuti, C. Catracchia and D. Pietrogiacomi, *Surf. Interfaces*, 2023, **42**, 103502.
8 M. C. Campa, A. M. Doyle, G. Fierro and D. Pietrogiacomi, *Catal. Today*, 2022, **384**–**386**, 76.
9 B. Bozorgi, J. Karimi-Sabet and P. Khadiv-Parsi, *Environ. Technol. Innovation*, 2022, **26**, 102344.
10 R. Li, Y. Li and Z. Liu, *Fuel*, 2024, **355**, 129405.
11 E. M. Kostyukhin, A. L. Kustov, N. V. Evdokimenko, A. I. Bazlov and L. M. Kustov, *J. Am. Ceram. Soc.*, 2021, **104**, 492.
12 Y. Wu, C. Dujardin, C. Lancelot, J. P. Dacquin, V. I. Parvulescu, M. Cabié, C. R. Henry, T. Neisius and P. Granger, *J. Catal.*, 2015, **328**, 236.
13 C. Huang, Y. Zhu, X. Wang, X. Liu, J. Wang and T. Zhang, *J. Catal.*, 2017, **347**, 9.
14 L. M. Kustov, E. M. Kostyukhin, E. Yu. Korneeva and A. L. Kustov, *Russ. Chem. Bull.*, 2023, **72**, 583.
15 A. A. Strekalova, A. A. Shesterkina, A. L. Kustov and L. M. Kustov, *Int. J. Mol. Sci.*, 2023, **24**, 8272.
16 Y. Wu, X. Ni, A. Beaurain, C. Dujardin and P. Granger, *Appl. Catal., B*, 2012, **125**, 149.
17 N. Russo, D. Mescia, D. Fino, G. Saracco and V. Specchia, *Ind. Eng. Chem. Res.*, 2007, **46**, 4226.
18 W. Y. Jung and S.-S. Hong, *J. Ind. Eng. Chem.*, 2013, **19**, 157.
19 N. A. Davshan, A. L. Kustov, O. P. Tkachenko, L. M. Kustov and C. H. Kim, *ChemCatChem*, 2014, **6**, 1990.
20 J. A. Villoria, M. C. Alvarez-Galvan, R. M. Navarro, Y. Briceño, F. Gordillo Alvarez, F. Rosa and J. L. G. Fierro, *Catal. Today*, 2008, **138**, 135.
21 X. He, M. Meng, J. He, Z. Zou, X. Li, Z. Li and Z. Jiang, *Catal. Commun.*, 2010, **12**, 165.
22 C. A. Chagas, F. S. Toniolo, R. N. S. H. Magalhães and M. Schmal, *Int. J. Hydrogen Energy*, 2012, **37**, 5022.
23 G. A. Tompsett, W. C. Conner and K. S. Yngvesson, *ChemPhysChem*, 2006, **7**, 296.
24 S. Horikoshi, A. Osawa, S. Sakamoto and N. Serpone, *Chem. Eng. Process.*, 2013, **69**, 52.

Received: 11th March 2024; Com. 24/7417